

Materials and methods

Chemicals: Purified rabbit polyclonal anti-Histone H4 antibody was purchased from *Abcam* (Cambridge, MA, USA). Affinity purified enhanced chemiluminescence (ECL) peroxidase-linked whole antibody anti-rabbit IgG from donkey was purchased from *GE Healthcare, Life Sciences* (Pittsburgh, PA, USA). (HMG)-CoA reductase assay kit and 4-(cytidine 5'-diphospho)-2-C-methyl-D-erythritol (CDP-ME) synthase assay kit were purchased from *Sigma-Aldrich* (St. Louis, USA) and *Echelon Biosciences Inc* (Salt lake city, UT, USA), respectively.

Immunoblotting: Total crude cell extract was prepared from leaves of the control and Gibberellin A₃ (GA₃)-treated tobacco plants at an early-vegetative growth stage (13 d after GA₃ application) using a plant total protein extraction kit (*Sigma*) following the manufacturer's instructions. Proteins (~50 µg) were electrophoresed on 15% (m/v) acrylamide gels and then transferred onto *Hybond-P* (*Amersham Biosciences*, Uppsala, Sweden) polyvinylidene difluoride (PVDF) membranes. After blocking the membrane in freshly prepared Tris-buffered saline + 0.1% (m/v) *Tween-20* (TBS-T) containing 5% (m/v) non-fat dry milk, the membranes were incubated with a polyclonal rabbit anti-histone H4 antibody at a dilution of 1:1 000 at 4 °C with agitation overnight, followed by incubation with an affinity purified donkey anti-rabbit HRP conjugated IgG antibody (*GE Healthcare, Life Sciences*) at a dilution of 1:5 000 for 1 h with agitation at room temperature. Immunoreactivity was detected and exposed to X-ray *HyperfilmTMECL* (*GE Healthcare, Life Sciences*) using an enhanced chemiluminescence, ECL detection system (*Thermo Fisher Scientific*, San Jose, USA) and visualized on a *Molecular Imager* chemiluminescence detection system (*ChemiDocTM XRS+*, *BioRad*, Hercules, USA). Equal loading of proteins was verified by Ponceau S staining of the membrane.

Measurement of *in vitro* enzyme activities: 3-hydroxy-3-methylglutaryl coenzyme A (HMG-CoA) reductase (HMGR) activity was determined based on spectrophotometric measurements (Baskaran *et al.* 2015). An HMGR assay kit from *Sigma-Aldrich* (St. Louis, MO, USA) with the catalytic domain of the human enzyme [a recombinant glutathione S-transferase (GST) fusion protein expressed in *E. coli*] was used under conditions recommended by the manufacturer to determine the *in vitro* effect of GA₃ on HMGR activity. The concentration of the purified human enzyme stock solution (*Sigma*) was 0.52-0.85 mg (protein) cm⁻³. A

reference statin drug pravastatin (*Sigma*) was used as a positive control, and distilled water as a negative control (blank). To characterize HMGR activity under defined assay conditions, a reaction containing 4 mm³ of NADPH (to obtain a final concentration of 400 µM) and 12 mm³ of the HMG-CoA substrate (to obtain a final concentration of 400 µM) in a final volume of 0.2 cm³ of 100 mM potassium phosphate buffer, pH 7.4 (containing 120 mM KCl, 1 mM EDTANa₂, and 5 mM dithiothreitol) was initiated (time 0) by the addition of 2 mm³ of the catalytic domain of human recombinant HMG-CoA reductase and incubated in an UV/Vis spectrophotometer (*Thermo ScientificTM MultiskanTM GO*, Hudson, New Hampshire, USA) equipped with a thermos-statically controlled cell holder) at 37 °C in the presence or absence (control) of 1 mm³ aliquots of GA₃ in a concentration range of 25, 50, and 100 mg dm⁻³. The rate of NADPH consumed was monitored every 20 s for up to 10 min by decrease in absorbance at 340 nm. Absorbance (A) was normalized to that of blank in each sample. Activation of HMGR [%] was calculated as $[A_{340} \text{ of treated} / (A_{340} \text{ of control} - 1)] \times 100$.

4-(cytidine 5'-diphospho)-2-C-methyl-D-erythritol (CDP-ME) synthase (IspD) activity: CDP-ME synthase activity was determined based on spectrophotometric measurements (Bernal *et al.* 2005) using a CDP-ME synthase assay kit (*Echelon Biosciences Inc*, UT, USA), as per manufacturer's recommendation. To determine and characterize the *in vitro* effect of GA₃ on CDP-ME synthase activity, Briefly, reaction contains 5 mm³ of methylerythritol phosphate (MEP) substrate (58 µM) and 10 mm³ of *IspD* (13.62 nM) in a final volume of 27 mm³ (harbouring 0.1 M Tris-HCl, pH 7.5, 1 mM MgCl₂, 0.2 mM CTP, 1 mM DTT and 44.5 mU cm⁻³ of auxillary enzyme, inorganic pyrophosphatase). A negative control (blank) contained all the components except the MEP substrate. Reaction was carried out at 30 °C and started by addition of 1 mm³ aliquots of GA₃ (in a concentration range of 0, 25, 50 and 100 mg dm⁻³). After 15 min of incubation, to each well, 100 mm³ of malachite green dye reagent was added. Plates were incubated at 30 °C under stirring for 15 min and absorbance at 630 nm was measured in a UV/Vis spectrophotometer plate reader. Absorbance was normalized to that of the blank in each sample. Phosphate standard (0-60 µM) prepared in a dilution buffer was quantified by colorimetric assay with malachite green as described above. A CDP-ME synthase inhibition [%] was calculated as $[(1 - A_{630} \text{ of treated}) / A_{630} \text{ of control}] \times 100$.

References

- Baskaran, G., Salvamani, S., Ahmad, S.A., Shahrudin, N.A., Pattiram, P.D., Shukor, M.Y.: HMG-CoA reductase inhibitory activity and phytochemical investigation of *Basella alba* leaf extract as a treatment for hypercholesterolemia. - *Drug.Des.Devel.Ther.* **9**: 509-517. 2015.
- Bernal, C., Palacin, C., Boronat, A., Imperial, S.: A colorimetric assay for the determination of 4-diphosphocytidyl-2-C-methyl-D-erythritol 4-phosphate synthase activity. - *Anal. Biochem.* **337**: 55-61, 2005.

Table 1 Suppl. List of primers used for quantitative real-time PCR (RT-qPCR) experiment (F - forward, R - reverse).

	Primers	Sequence (5'-3')	Accession No.	Target gene	T _m [°C]	Primer length [bp]	Amplicon length [bp]
House-keeping	IME1079F	CGCGCTACACTGATGTATTC	AJ236016	<i>Nt18SrRNA</i>	52	20	170
	IME1079R	GTACAAAGGGCAGGGACGTA			54	20	
GA signaling	IMN1078F	AAGCCCATGGTTGTTGAGAC	XM_009784954	<i>NtEF-1 α</i>	51.8	20	105
	IMN1078R	GTCAACGTTCTTGATAACAC			47.7	20	
MVA pathway	GA20ox1-F	TGTAGCACGAGAACTTCC	AB109762	<i>NtGA20ox1</i>	48.04	18	106
	GA20ox1-R	ACGGCATGCTTCACCAACA			51.09	19	
	GA20ox2-F	TGAGGTTCCCTTTCACAGCA	XM_009773318.1	<i>NtGA20ox2</i>	52.4	21	145
	GA20ox2-R	CTCCCCTAAAAGCTCCATTACC			54.84	22	
	GA20ox2-F	CGTTCAATTTCTTTGCCAC	AB125233.1	<i>NtGA20ox2</i>	49.73	20	87
	GA20ox2-R	GCAGTTGTCTTTGGAGAAGTGC			54.84	22	
	GA20ox3-F	TGAGGTTCCCTTTCACAGCA	EF471117.1	<i>NtGA20ox3</i>	49.73	20	95
	GA20ox3-R	GCTATCTATAGGAAATCCAATG			49.25	22	
	GA20ox5-F	ATCCATCGCTATTCGCCGA	EF471118.1	<i>NtGA20ox5</i>	51.09	19	102
	GA20ox5-R	GCTATCTTTCCAGCGCCAA			51.78	20	
MEP pathway	AACT1-F	TTGGGCATCAATGATGTTGTGG	AY748245.1	<i>NtAACT1</i>	55.27	23	274
	AACT1-R	GAGCAGCGATGCCACGTTCAAA			56.7	22	
	HMGR1-F	TTGGCATCGGATTTGTTCCAG	U60452	<i>NtHMGR1</i>	49.73	20	105
	HMGR1-R	GGCGGTATCTTCCTCAAT			51.09	19	
	MVD-F	TTAGGAAAATTCGCGCTCGT	KJ808764.1	<i>NtMVD</i>	51.78	20	144
	MVD-R	CAGCTGAGGAGGCCAAACCC			57.93	20	
	FPPS-F	CTTCTCCGCAACCACATCAC	GQ410573	<i>NtFPPS</i>	53.83	20	107
	FPPS-R	GAGGCAGTCTGGAACCAACC			56.31	21	
	SQS-F	AGGAGGTGGAAACAACCTGATGA	U60057	<i>NtSQS</i>	52.97	22	213
	SQS-R	AGAACATACGGCACTTGGGT			51.78	20	
Shikimate pathway	GDS-F	AGTTGGACATCAGTTGAACAAGAA	XM_009593283.1	<i>NtGDS</i>	52.76	25	154
	GDS-R	ATAAAGGCATTCTTTATTACGTCTTCC			54.06	28	
	IspE-F	CAAAAAACCCACATTGGTTCTTTAA	KJ159923.1	<i>NtIspE</i>	55.18	27	187
	IspE-R	CTTCTTCAGGATTATGTTATCTC			53.66	27	
	β-LCY1-F	GCCTGTATCTTCTGAGCTTATATTTTC	KC484706	<i>NtLcyB1</i>	57.27	29	289
	β-LCY1-R	TCAGAAAATGGAAATAGTTACTATTGCAAT			53.42	30	
	ε-LCY-F	CAGGAGTCTTTTCGAGGAAACTTG	KC484707	<i>NtLcyE</i>	56.04	25	358
	ε-LCY-R	GTGTTCCAAGCTTGAGTTGAGAT			53.49	23	
	β-Ohase-F	ATGGCCGCCAGCAGAATTTTC	JX101477	<i>NtBCH2</i>	53.83	20	252
	β-Ohase-R	CTCAATTTTCATTTCATCTCCTCTGTC			55.53	28	
Phenylpropanoid pathway	DHQ/SDH-F	GGGGCTGTCAATTGTGTCTGCT	AY578144.1	<i>NtDHQ/SDH</i>	53.83	20	
	DHQ/SDH-R	CTCGTTTCATAGGTACGGTT			48.93	19	
	ASA1-F	AATGATGTAGGAAAAGGTGTC	XM_009614484.1	<i>NtAsa1</i>	48.5	21	136
	ASA1-R	CATCCCAACAGGTTAAATG			46.77	19	
	ASA2-F	TACATACAAGCCAGAGGCTG	AF079168.1	<i>NtAsa2</i>	51.78	20	134
	ASA2-R	ATCACATCCTCATCAGGTGT			49.73	20	
	TSA-F	TGAGAGATGCTGGGTGATACAT	XM_009786553.1	<i>NtTSa</i>	49.73	20	320
	TSA-R	TGCCACCTGTTGACATGCT			51.78	20	
Ethylene signaling	PAL-F	GCAAACAGCTCAATCTTCCA	D17467	<i>NtPAL</i>	49.7	20	74
	PAL-R	TCGACTTCTTTTGCCAACAC			49.7	21	
Auxin signaling	ACS1-F	GACCTTCACCAACCAAC	X65982	<i>NtACS1</i>	47.05	17	553
	ACS1-R	ATCCTGGCTCTTGACAATC			48.93	19	
Sugar metabolism	IA1C-F	TCCTCTTAGACTACCAGACA	X83229	<i>NtIA1C</i>	49.73	20	416
	IA1C-R	GGTGATTGCTCAGCTGAT			51.09	19	
Sugar metabolism	YUCCA4-F	GCAGGTCTTCTGGTTTAGCA	XM_006353587.2	<i>StYUCCA4</i>	54.4	21	66
	YUCCA4-R	CAAGAATGAGTGAAGGGACTCCAT			55.7	24	
Sugar metabolism	GH3.6-F	GCTATTAGCAATGGTGCTTC	XM_009781249.1	<i>NsGH3.6</i>	49.73	20	145
	GH3.6-R	ATTGCTTGTGACCAGGAACC			51.78	20	
	AMY1-F	CGACTCTTTTCTAAGCAAGTAAACG	FS438032	<i>NtAMY1</i>	54.81	26	118
	AMY1-R	GCGTATCACAACCAGTGGATCA			54.84	22	
	Inv-F	CGGATATTATGCCCGATGA	KF308284.1	<i>NtInv</i>	48.93	19	255
	Inv-R	CTGCCTTGTCCAAACTTGC			51.09	19	
	SPS-F	GGTGGTCAGGTGAAGTATGTTG	KJ544563.1	<i>NtSPS1</i>	54.84	22	418
	SPS-R	CATTTAAAGCACCTGACAG			46.77	19	
	SUS-F	CACGGATATTTGCCCCAGGA	AB055497.1	<i>NtSUSY</i>	53.83	20	203
	SUS-R	GCAGCAGCCGAGTAGCAATA			53.83	20	
Sugar metabolism	GBSS-F	TCAAATAATAGTCTTGGAACTGG	AB028026.1	<i>NtGBSS</i>	52.26	24	103
	GBSS-R	ATTGAATTTTGCCGCTCCTTTAG			51.71	23	
	MST1-F	TTGCTTGGTCTGGGGACC	X66856.1	<i>NtMST1</i>	55.41	19	201
	MST1-R	CAGTCATAATCACAACAAAGAAT			48.14	23	

	PFK-F	CAATTTAAAGGACAGTTCAC	EU099316.1	<i>NtPFK</i>	48.5	21	193
	PFK-R	GTGCTGTCCACCTACGGTCA			56.31	21	
	PGK-F	TGGCGGTGAAGAAGAGCGTGGGA	Z48976.1	<i>NtPGK</i>	60.62	23	203
	PGK-R	AGGGCGACCAAGATGAGAGGCAA			58.84	23	
	PGM-F	GAATTACAAGGTCTTAATAAGCA	XM_009764206.1	<i>NsPGM</i>	48.14	23	201
	PGM-R	CCCATGGGCAGCGATCAT			52.6	18	
	PK-F	TATTGACATGATTGCGTTATCT	Z29492.1	<i>NtPK</i>	47.38	22	184
	PK-R	CAGGTCACCTCTTGCCACC			55.41	19	
	PDH1-F	TATGGAATGGGGACAGCAG	AB090281.1	<i>NtPDH1</i>	51.09	19	72
	PDH1-R	AGGAAACATAATCTCCTCTTT			45.63	20	
	G6PD-F	GTCAACTGTTCAAAGTGAATT	AJ001770.1	<i>NsG6PD</i>	46.55	21	177
	G6PD-R	ATTCTATGCAAAAAGTGGGG			46.77	19	
	PGL1-F	GTCGGGCCTGACTGTCCGTTGTC	XM_009614389.1	<i>Nt6PGL1</i>	62.4	23	411
	PGL1-R	GAACAATAGGGACCTTGATAAAAATCCA			57.27	29	
	6PGD-F	GCTGAGGGCAAAGAGTGCT	XM_009791594.1	<i>Ns6PGD</i>	53.25	19	100
	6PGD-R	ATCCAAGAACACTGCCCTG			51.09	19	
	MCCB-F	AACTGTATGGCACTACACTTGT	XM_009632683.1	<i>NtMCCb</i>	51.11	22	174
	MCCB-R	ATCCAGTAATATTCTGAAGAAAGATCA			52.14	27	
	ACLA2-F	GTGCTCCACTTGTGCGGACA	XM_009801273.1	<i>NsACAL2</i>	55.88	20	359
	ACLA2-R	ACTAGCTCCTCCACCAGCAA			53.83	20	
	ACS-F	GGTTCTGCTACTTTTCCTTT	XM_009803880.1	<i>NsACS</i>	47.68	20	429
	ACS-R	TTTTCGCAGGTCATCACTGT			47.73	20	
	MDH1-F	CACCCCAAAGGCAAATTTGG	KJ730262.1	<i>NtMDH</i>	51.78	20	376
	MDH1-R	ATTGTGTTAGCAAATTTGAT			44.6	21	
	IDH-F	AAAAATCCGCGTTGAAAAATCCT	X96728.1	<i>NtIDH</i>	48.5	21	117
	IDH-R	ATACTTCGTATCCAACCTAG			48.5	21	
	PEPCase-F	ATGGGATGCATCCACCCGT	X59016.1	<i>NtPEPCase</i>	53.25	19	193
	PEPCase-R	GGTTTACGCTTTGATGGACGGCT			57.06	23	
Epigenetics	MTCBP-F	TGCCCTGAGAACTACCGAATTA	XM_009770876.1	<i>NsMTCBP</i>	53.49	23	360
	MTCBP-R	AGCAGCAGCATTAACTGCACAGC			57.06	23	
	SAMS-F	CCTCAGAATCAGTTAACGAAGGG	AY445582	<i>NtSAMS</i>	55.27	23	89
	SAMS-R	TGGATCTTGTCTAGGCAAGCG			54.84	22	
	HMT1-F	TGGAAGCTGGCGCAGATATA	XM_009801399.1	<i>NsHMT1</i>	51.78	20	162
	HMT1-R	TTCTTTTCACTACATTCCAG			45.63	20	
	SAHH-F	GCGAAAAACAAATCGACAGAGG	D45204.1	<i>NtSAHH</i>	52.4	21	90
	SAHH-R	AAATACTAGTATCCTAAACAAAATC			47.84	25	
	MS1-F	GTAGACACTGTTCCAGTCCT	XM_009621138.1	<i>NtMS1</i>	51.78	20	394
	MS1-R	CTTTGATCAAATCAAGGGTCTG			51.11	22	
	SET1-F	GAGTTACAAAACCTTGATACAT	AJ294474.1	<i>NtSet1</i>	47.38	22	93
	SET1-R	CGAGCTTTAGGACCTCCTTGAG			56.7	22	
	MET1-F	TGAACCAGAAGACAAGCCGTAGT	AB030726.1	<i>NtMET1</i>	59	23	73
	MET1-R	ATCTCATCCTCATTGATCTTGATGTA			58	27	
	DRM1-F	AGACCGCTTGGAGCAACTGATA	AB087883.1	<i>NtDRM1</i>	60	22	66
	DRM1-R	CACGGGCTTCCACCAATTA			58	19	
	CMT3-F	CCAGAGACTGCGGTAAGAAATGA	AB032538.1	<i>NtCMT3</i>	59	23	65
	CMT3-R	TGCCTCCACTCCCTCAAAAG			59	20	
	ROS1-F	GATCGGCTACAGCTAATGCAGC	AB281587.1	<i>NtROS1</i>	56.7	22	389
	ROS1-R	TCCTTGTGCTCCTACATTAGGC			54.84	22	
	HAT1-F	AGGCGGTGCTGATTCCGACT	AB723510.1	<i>NtHAT</i>	55.9	20	87
	HAT1-R	TTGCGCATGGAAGAGCCATCGT			56.7	22	
	HD2a/b-F	AGGAAGGCAGATTCCGGCTACA	FJ903174.1/	<i>NtHD2a/b</i>	54.36	21	165
	HD2a/b-R	TGATTTTGGAGTCTGCTGGTT	FJ903175.1		50.45	21	
Cell wall	CwINV5-F	AATAAAAAAATAACACAGGAATTGGT	HM022267.1	<i>NtCwInv5</i>	49.11	27	140
	CwINV5-R	ATTGTTGAACTGGGAAAAAATC			48.14	23	
	CeSA-F	CCCTCATGCCTCAGATAA	XM_009611332.1	<i>NtCeSA</i>	48.04	18	53
	CeSA-R	GAATACCGGTGATTGTCCAA			49.73	20	
	CALS3-F	CAGTGCGAATCTCCAACCTCGT	XM_009781239.1	<i>NsCSL3</i>	54.36	21	161
	CALS3-R	CCAGAAGCATGCCCCAGC			54.88	18	

Table 2 Suppl. Gas chromatography with mass spectrometry analysis of different compounds. Means \pm SDs, $n = 3$. Asterisks indicate significant differences at $P < 0.05$. RT - retention time, M.M. - molecular mass, RFC - relative fold change.

Compound name	RT [min]	Formula	M.M.	RFC [peak area]
2-Methoxy 4-vinyl phenol	20.608	C ₉ H ₁₀ O ₂	150.18	4.77 \pm 0.16*
Nicotine	24.284	C ₁₀ H ₁₄ N ₂	162.23	25.53 \pm 0.15*
Solanone	25.013	C ₁₃ H ₂₂ O	194.31	3.41 \pm 0.15*
Mysomine	27.331	C ₉ H ₁₀ N ₂	160.21	38.99 \pm 4.77*
Farnesol	27.611	C ₁₅ H ₂₆ O	222.37	6.41 \pm 0.68*
Geranyl acetone	28.61	C ₁₃ H ₂₂ O	196.29	26.54 \pm 0.21*
3-Hydroxy- β -damascone	34.91	C ₁₃ H ₂₀ O ₂	208.29	18.94 \pm 0.86*
Megastigmatrienone-III	35.287	C ₁₃ H ₁₈ O	190.28	102.12 \pm 3.12*
3-Oxo- α -ionol	36.039	C ₁₃ H ₂₀ O ₂	208.30	9.37 \pm 0.24*
Cotinine	38.157	C ₁₀ H ₁₂ N ₂ O	176.21	28.19 \pm 0.3257*
Tetradecanoic acid	40.282	C ₁₄ H ₂₈ O ₂	228.37	17.23 \pm 0.47*
Solavetione	41.641	C ₁₅ H ₂₂ O	218.34	5.94 \pm 0.24*
Rishitin	42.255	C ₁₄ H ₂₂ O ₂	222.32	52.72 \pm 6.30*
Neophytadiene	42.986	C ₂₀ H ₃₈	278.51	6.01 \pm 0.02*
Isolimonene	43.829	C ₁₀ H ₁₆	136.23	57.77 \pm 1.41*
Hexadecanoic acid methyl ester	45.837	C ₁₆ H ₃₂ O ₂	256.42	23.66 \pm 0.40*
Scopoletin	46.637	C ₁₀ H ₈ O ₄	192.17	41.96 \pm 1.75*
Pentadecanoic acid	47.276	C ₁₅ H ₃₀ O ₂	242.39	8.82 \pm 0.25*
Glucyl alcohol	48.111	C ₁₅ H ₂₄ O	220.35	23.55 \pm 0.57*
Stearic acid	48.348	C ₁₈ H ₃₆ O ₂	248.47	201.62 \pm 2.26*
Phytol	50.297	C ₂₀ H ₄₀ O	296.53	21.66 \pm 1.07*
4,8,13-Duvatriene-1,3-diol (DVT)	51.765	C ₂₀ H ₃₄ O ₂	306.48	21.04 \pm 0.16*
Longifolenaldehyde	54.298	C ₁₅ H ₂₄ O	220.35	28.14 \pm 1.311*
Squalene	70.282	C ₃₀ H ₅₀	410.71	1.21 \pm 0.19
β -Tocopherol	76.9	C ₂₈ H ₄₈ O ₂	416.68	120.73 \pm 10.75*
Campesterol	78.606	C ₂₈ H ₄₈ O	400.68	33.71 \pm 1.83*
Stigmasterol	79.348	C ₂₉ H ₄₈ O	412.69	20.11 \pm 0.27*
β -Sitosterol	80.498	C ₂₉ H ₅₀ O	414.70	25.01 \pm 0.91*
Cholestrol	81.026	C ₂₇ H ₄₆ O	386.65	89.87 \pm 2.92*
Vitamin E	82.97	C ₂₉ H ₅₀ O ₂	430.70	29.14 \pm 1.08*

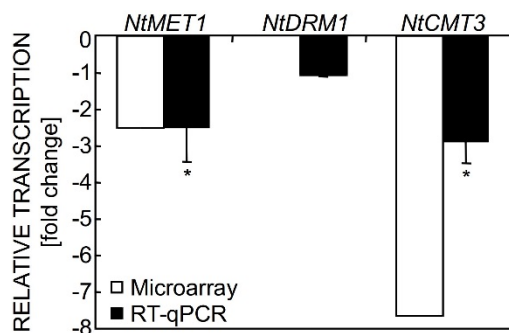


Fig. 1 Suppl. Effect of GA₃ application on relative transcription of DNA methyl transferase (*NtDNMT*) genes: *NtMET1*, *NtDRM1*, and *NtCMT3* (with normalization to an endogenous housekeeping gene encoding elongation factor 1- α (*EF1- α*) RNA) determined by RT-qPCR analyses of control and GA₃-treated tobacco leaves (13 d after GA₃ application). The data analyzed by RT-qPCR ($2^{-\Delta\Delta C_T}$) and microarray are depicted as relative fold-changes (RFC) in the gene transcription. Comparison of microarray (empty bars) and RT-qPCR analysis (filled bars) of differential expressed genes. The value of each corresponding gene for the control sample was set to 1. Since the RFC < 1, thereby the reciprocal was taken. Notably, the transcript level of *NtDRM1* was not detected in the microarray experiment. Means \pm SDs, $n=3$. Asterisks indicate significant differences at $P < 0.05$.



Fig. 2 Suppl. Immunoblotting of nuclear extracts from control (untreated, U) and GA₃-treated (T; 13 d after application) using an anti-histone H4 antibody. Nuclear extracts were prepared using a *CellLyticTMPN* plant nuclei isolation/extraction kit (*Sigma*) following the manufacturer's instructions. Nuclear extracts quality was assessed by Western blot analysis using an anti-histone antibody directed against the histone H4. Approximately 50 μ g of the nuclear extract was separated by 15% (m/v) SDS-polyacrylamide gel electrophoresis and probed with the anti-histone H4 antibody. Equal loading of proteins was verified by Ponceau S staining the membrane.

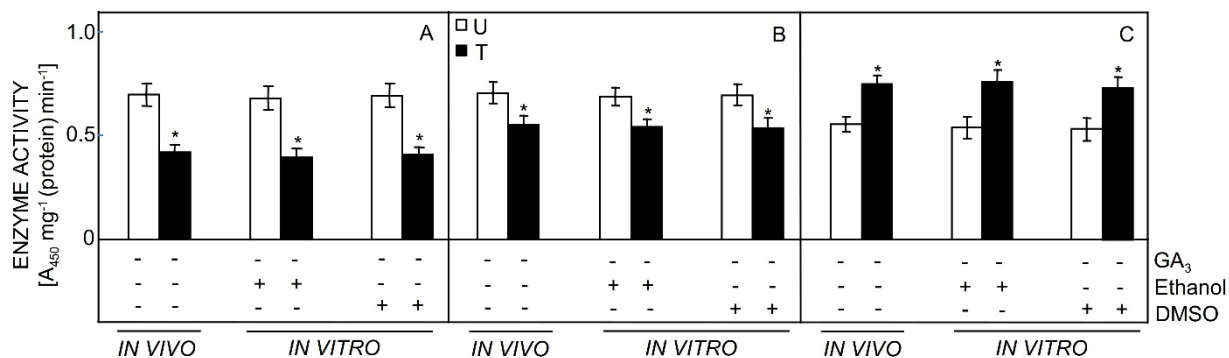


Fig. 3 Suppl. Effect of solvents (ethanol and dimethyl sulfoxide, DMSO) on DNA methyltransferases (NtDNMTs), histone acetyltransferases (NtHATs) and histone deacetylases (NtHDACs) activities. Nuclear extracts were prepared using a *CellLyticTMPN* plant nuclei isolation/extraction kit (*Sigma*) following the manufacturer's instructions. Total NtDNMT (A), NtHDAC (B), and NtHAT (C) activities from the nuclear extract of control (U) and GA₃-treated (T) samples were determined using an ELISA based colorimetric assay kit. Total enzymatic activities after *in vitro* addition of ethanol (GA₃ solvent) and DMSO (solvents of inhibitors of DNMTs, HATs, and HDACs) to a final conc. of 0.01% (v/v) in nuclear extracts were also measured. Means \pm SDs, $n = 3$; asterisks indicate significant differences at $P < 0.05$.

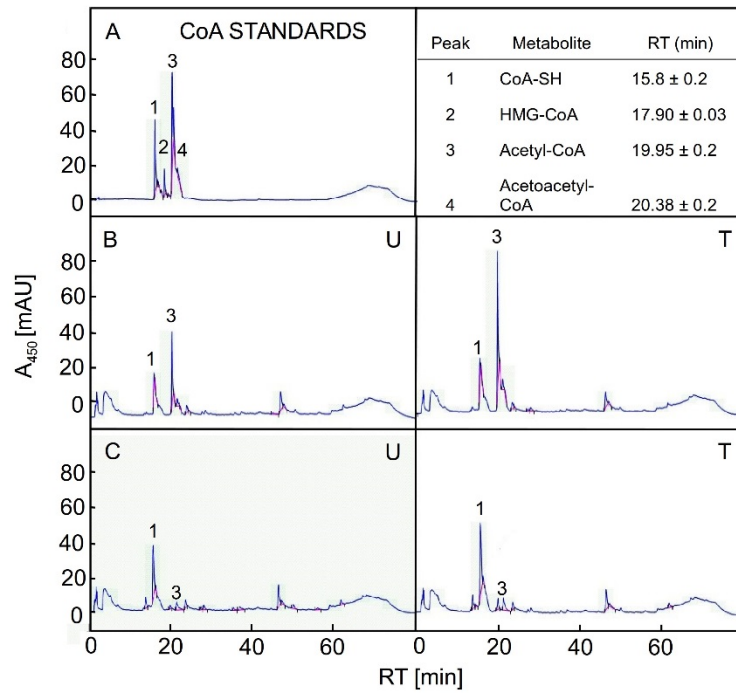


Fig. 4 Suppl. A typical chromatographic separation of coenzyme A (CoA) standards and trichloroacetic acid (TCA) soluble extracts. *A* - Representative HPLC chromatogram illustrating separation of various CoA compounds. *B*, *C* - Representative chromatograms showing the separation of TCA soluble extracts before (*B*) and after (*C*) 14.53 M NH_4OH treatment for 15 min. Peaks corresponding to CoA-SH and acetyl-CoA were detected and their corresponding areas were determined. U - , T - GA₃ treated tobacco, RT - retention time, CoA-SH - coenzyme A (reduced), HMG-CoA - 3-hydroxy-3-methylglutaryl coenzyme A.

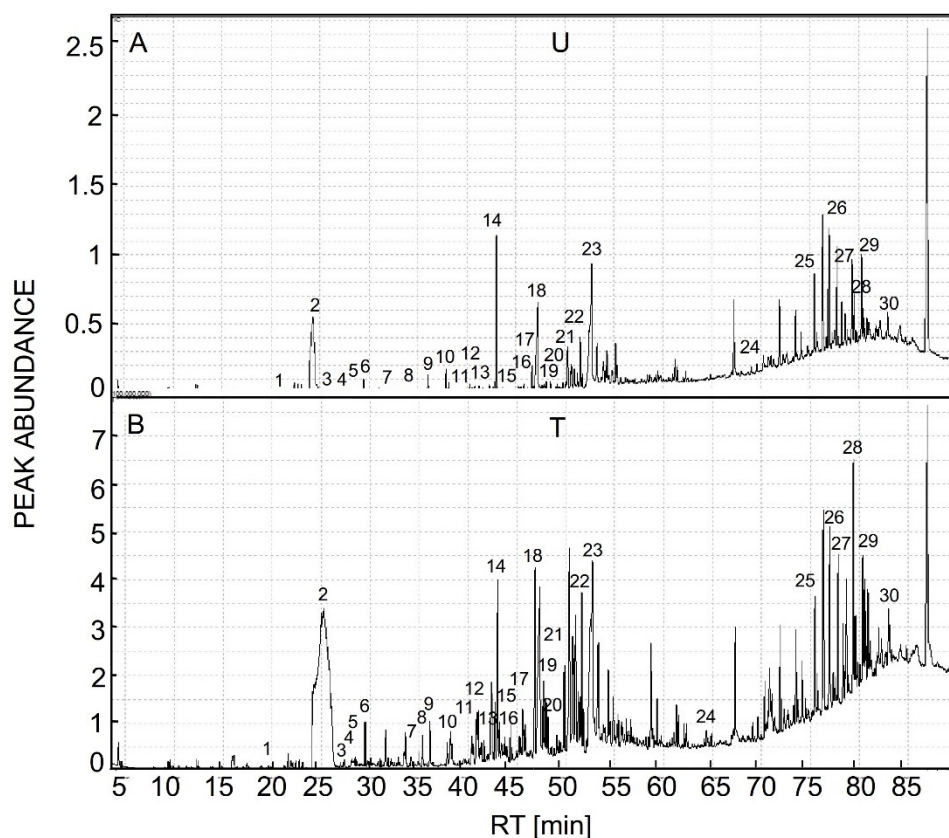


Fig. 5 Suppl. A representative GC-MS chromatogram of dichloromethane (DCM) extracts. Peak identification with retention times (RT): 2-methoxy 4-vinyl phenol, 20.608 min (1), nicotine, 24.284 min (2), solanone, 25.013 min (3), mysomine, 27.331 min (4), farnesol, 27.611 min (5), geranyl acetone, 28.61 min (6), 3-hydroxy- β -damascone, 34.91 min (7), megastigmatrienone-III, 35.287 min (8), 3-oxo- α -ionol, 36.039 min (9), cotinine, 38.157 min (10), tetradecanoic acid, 40.282 min (11), solavetione, 41.641 min (12), rishitin, 42.255 min (13), neophytadiene, 42.986 min (14), isolimonene, 43.829 min (15), hexadecanoic acid, methyl ester, 45.837 min (16), scopoletin, 46.637 min (17), pentadecanoic acid, 47.276 min (18), glaucyl alcohol, 48.111 min (19), stearic acid, 48.348 min (20), phytol, 50.297 min (21), DVT, 51.765 min (22), longifolenaldehyde, 54.298 min (23), squalene, 70.282 min (24), β -tocopherol, 76.9 min (25), campesterol, 78.606 min (26), stigmasterol, 79.348 min (27), β -sitosterol, 80.498 min (28), cholesterol, 81.026 min (29), and Vitamin E, 82.97 min (30). U - Untreated, T - GA₃ treated tobacco. Quantitative analysis of aforementioned identified metabolites is depicted in Table 2 Suppl.

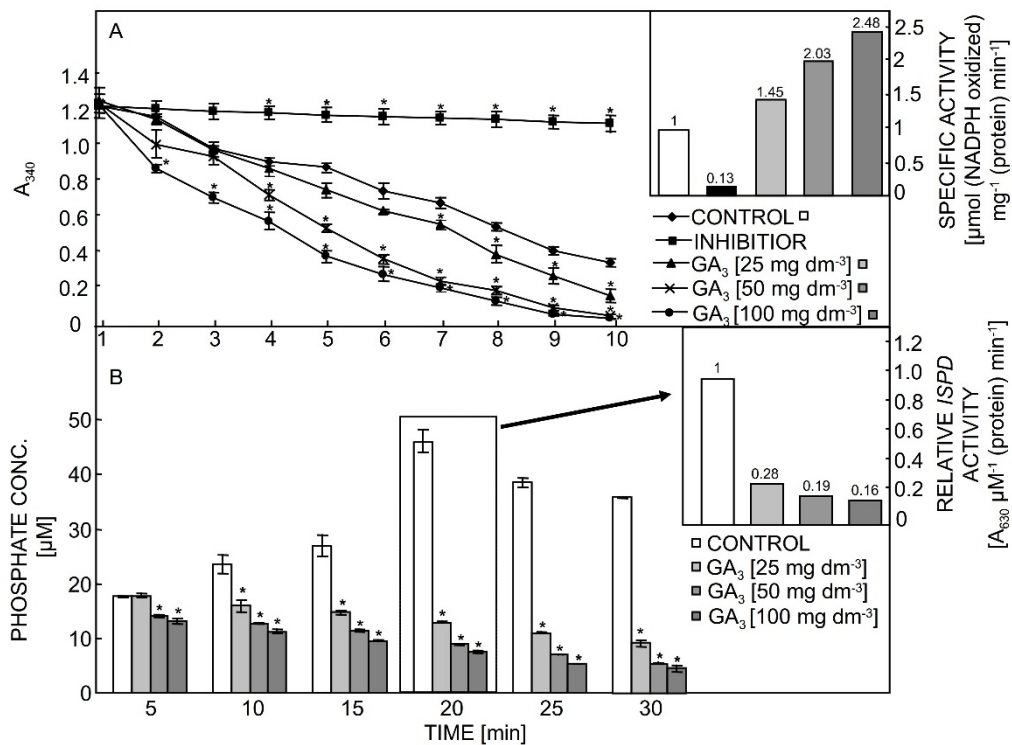


Fig. 6 Suppl. Effect of *in vitro* GA₃ addition on 3-hydroxy-3-methylglutaryl coenzyme A (HMG-CoA) reductase (HMGR) and 4-(cytidine 5'-diphospho)-2-C-methyl-D-erythritol (CDP-ME) synthase (IspD) activities. A - HMGR activation. Direct activation of the catalytic domain of human HMGR in a cell-free assay by *in vitro* GA₃ treatment was performed using a HMGR assay kit (*Sigma-Aldrich*). A reaction containing 4 mm³ of NADPH and 12 mm³ of the catalytic domain of human recombinant HMG-CoA reductase and incubated in quartz microcells at 37 °C in the absence (control) or presence of 1 mm³ aliquots of GA₃ (dissolved in ethanol) harboring varying concentrations (25, 50, and 100 mg dm⁻³). The rate of NADPH consumed was monitored for up to 10 min by recording the decrease in absorbance at 340 nm. Absorbance was normalized to that of blank for each sample. The resulting reaction curves demonstrated the ability of GA₃ to enhance HMGR activity. The concentration of the enzyme stock solution was 0.6 mg (protein) cm⁻³ and the specific activity of untreated (U) and GA₃-treated (T) samples in the presence of a 400 μM HMG-CoA substrate calculated between 20-300 s was 1.67±0.22 and 4.55±0.04 μmol of NADPH oxidized mg⁻¹ (protein) min⁻¹, respectively. Means ± SDs, n = 3, asterisks indicate significant differences at P < 0.05. The inset depicts a GA₃ induced fold-change in HMGR specific activity relative to control specific activity of the enzyme in the absence of GA₃. Empty and filled bars indicate U and T samples, respectively. B - CDP-ME synthase (IspD) suppression. Effect of GA₃ treatment on the CDP-ME synthase activity in a cell-free assay *in vitro* was determined using a CDP-ME synthase assay kit (*Echelon Biosciences*). A reaction was performed harboring 5 mm³ of MEP substrate (58 μM) and 10 mm³ of CDP-ME synthase (13.62 nM) in a final volume of 27 mm³ of reaction mixture, containing 0.1 M Tris-HCl, pH 7.5, 1 mM MgCl₂, 0.2 mM CTP, 1 mM DTT, 3.75 μM purified CDP-ME synthase, and 44.5 mU cm⁻³ of inorganic pyrophosphatase, in quartz microcells at 30 °C in the absence (control) or presence of 1 mm³ aliquots of GA₃ (dissolved in ethanol) of varying concentrations (25, 50, and 100 mg dm⁻³). The formation of CDP-ME occurs at a 1:1 and a 1:2 ratio with the formation of PP_i and free phosphate, respectively, in the presence of pyrophosphatase. By measuring free phosphate content, amount of MEP converted to CDP-ME was inferred. The rate of inorganic phosphate released was determined colorimetrically with malachite green by spectrophotometric scanning at 630 nm for up to 30 min, resulted in the depicted bar graphs. The standard stock solution of phosphate (at a concentration range of 0 - 60 μM) was also subjected to malachite green based colorimetric estimation. A linear calibration curve was obtained by fitting the absorbance of samples against the standard concentration. The specific activity (absorbance) of U and T samples calculated after 20 min of reaction was 1.32 ± 0.06 and 0.22 ± 0.01 μmol¹ (protein) min⁻¹, respectively. All assays were performed with three technical replicates. Empty and filled bars indicate U and T samples, respectively. Means ± SDs, n = 3. Asterisks indicate significant differences at P < 0.05. The inset depicts a GA₃ suppressed fold-change in CDP-ME synthase specific activity relative to a control.

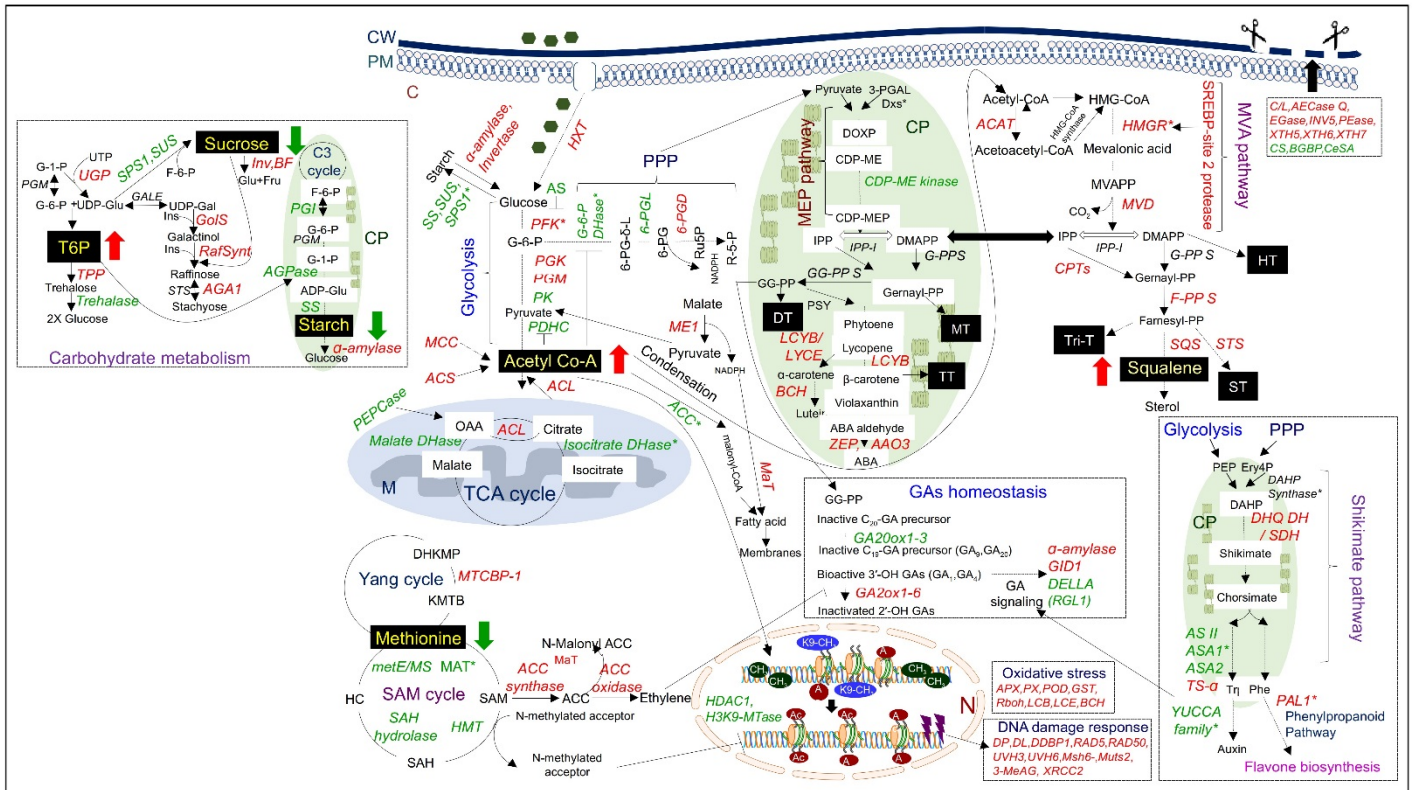


Fig. 7 Suppl. A schematic view of GA₃ induced transcriptional networks and metabolic pathways and their interconnections based on microarray and limited metabolite profiling. Key genes/enzymes are shown in either red- or green-arrows representing their corresponding up- or down-regulation, respectively. Gibberellin A₃ (GA₃) application causes the suppression of S-adenosylmethionine (SAM) cycle, endogenous GAs, biosynthesis, TCA cycle/oxidative phosphorylation, and upper 2-methyl-D-erythritol-4-phosphate/1-deoxy-D-xylulose-5-phosphate (MEP/DOX) pathway (feeding module) with concomitant activation of sugar metabolism, ethylene and ABA biosynthesis, glycolysis, mevalonate (MVA) pathway, shikimate/phenylpropanoid pathway, fatty acids biosynthesis, and cell wall catabolism. Application of GA₃ leads to an increase in cellular acetyl-CoA pool and its probable metabolic shift towards secondary metabolism as characterized by a concomitant increased accumulation of phytochemicals, total flavonoid content (TFC) and total phenolic content (TPC). Apart from these, other genes that are involved in oxidative stress, DNA repair, and cellular stress response are also shown.

DEGs (differentially expressed genes) are as follows: *3-MeAG* - DNA-3-methyladenine glycosylase, *6-PGD* - 6-phosphogluconate dehydrogenase, *6-PGL* - 6-phosphogluconolactonase, *ACAT* - acetyl-coenzyme A acetyltransferase, *ACC oxidase* - 1-aminocyclopropane-1-carboxylate oxidase, *ACCS* - 1-aminocyclopropane-1-carboxylate synthase, *ACCo** - acetyl-CoA carboxylase, *ACL* - ATP-citrate lyase, *ACS* - acetyl-CoA synthetase, *AECCase Q* - acidic endochitinase Q, *ALDHs* - alcohol dehydrogenases, *APX* - ascorbate peroxidase, *AS* - ATP synthase (β-subunit or γ-chain), *ASA1** - anthranilate synthase α-1, *ASA2* - feedback-insensitive anthranilate synthase α-2 chain, *ASII* - anthranilate synthase component II, *BCH* - β-carotene hydroxylase, *BGBP* - β-glucan-binding protein, *C/L* - chitinase/lysozyme, *CDP-ME kinase* - 4-(cytidine 5'-diphospho)-2-C-methyl-D-erythritol kinase, *COX15* - cytochrome c oxidase assembly protein, *CPTs* - cis-prenyltransferases, *CS* - callose synthase, *DAHPh synthase* - 3-deoxy-D-arabinoheptulosonate 7-phosphate synthase, *DDBP1* - DNA damage-binding protein 1, *DHQ dehydratase/SDH* - 3-dehydroquinate dehydratase/shikimate dehydrogenase isoform, *DL* - DNA ligase, *DMRPs* - DNA mismatch repair proteins viz. *Msh6-1* and *Muts2*, *DP* - DNA photolyase, *DRH* - DNA repair helicase viz. *UVH6*, *DRPs* - DNA-repair proteins viz. *RAD5*, *RAD50*, and *UVH3*, *EGase* - endo-1,4-β-glucanase/endo-β-1,3-glucanase, *F-PP synthase* - farnesyl-PP synthase, *G-6-P DHase** - glucose-6-phosphate dehydrogenase, *GA20ox* - gibberellin 20-oxidase 1, *GA2ox* - gibberellin 2-oxidase 2, *GG-PP synthase* - geranyl-geranyl-PP synthase, *GID* - gibberellin insensitive dwarf 1, *GSTs* - glutathione S-transferases, *H3K9-MTase* - histone H3-lysine 9 methyltransferase, *HMGR** - HMG-CoA reductase, *HMT* - L-homocysteine S-methyltransferase, *INV5* - cell wall invertase, *Isocitrate DHase* - isocitrate dehydrogenase, *LCYB* - lycopene β-cyclase, *LCYE* - lycopene ε-cyclase, *Malate DHase* - malate dehydrogenase, *MaT* - malonyltransferase, *MAT* - S-adenosylmethionine synthase (methionine adenosyltransferase), *MCC* - 3-methylcrotonyl-CoA carboxylase, *ME1* - NADP-dependent malic enzyme, *metE* - 5-methyltetrahydropteroyltri-glutamate-homocysteine S-methyltransferase, *MS* - methionine synthase, *MTCBP-1* - 1,2-dihydroxy-3-keto-5-methylthiopentane dioxygenase 1, *MVD* - mevalonate-5-pyrophosphate decarboxylase, *NAPRT* - nicotinate phosphoribosyltransferase-like protein, *NASI* - nicotianamine synthase 1, *NUP1/2* - nicotine uptake permease 1/2, *PX* - peroxidase, *PAL1** - phenylalanine ammonia-lyase 1, *PDHC* - pyruvate dehydrogenase complex (E3 subunit), *PEase* - pectinesterase, *PEPCase* - phosphoenolpyruvate carboxylase 1, *PFK** - phosphofructokinase, *PGK* - phosphoglycerate kinase, *PGM* - phosphoglyceromutase, *PK* - pyruvate kinase, *PSY* - phytoene

synthase, *Rboh* - respiratory burst oxidase homologs, *RGL* - repressor of GA1-3 (*RGA*) like, *ROSI* -repressor of silencing 1, *SAH hydrolase* - S-adenosyl-homocysteine hydrolase, *SPSI** - sucrose-phosphate synthase 1, *SQS* - squalene synthase, *SS* - starch synthase, *SUS* - sucrose synthase, *STS* - sesquiterpene synthase, *TPP* - trehalose pyrophosphatase, *TS-a*- tryptophan synthase α -subunit, *UGP* -UTP-glucose-1-phosphate uridylyltransferase, *XRCC2* - X-ray repair cross complementing protein 2, *XTH* - xyloglucan endotrans-glucosylase/hydrolase, and *YUC1-5** - YUCCA family. Notably, an *asterisk* indicates a rate-limiting enzyme in corresponding metabolic pathways.

Different metabolites are as follows: 3-PGA - 3-phosphoglycerate, 6-PG - 6-phospho-D-gluconic acid, ABA - abscisic acid, ACC - 1-aminocyclopropane-1-carboxylate, CDP-ME - 4-(cytidine 5'-diphospho)-2-C-methyl-D-erythritol, CDP-MEP - 4-(cytidine 5'-diphospho)-2-C-methyl-D-erythritol 4-phosphate, DAHP - 3-deoxy-D-arabinoheptulosonate 7-phosphate, DHKMP - 1,2-dihydro-3-keto-5-methylthiopentene, DMAPP - dimethylallyl diphosphate, DNMT1 - DNA (cytosine-5-)-methyltransferase 1, DT - diterpenes, DOXP - deoxyxylulose 5-phosphate, ERY4P - erythrose 4-phosphate, FPP - farnesyl diphosphate, G-6-P - glucose 6-phosphate, GGPP - geranylgeranyl diphosphate, GPP - geranyl diphosphate, HC -homocysteine, HT - hemiterpene, IPP - isopentenyl diphosphate, KMTB - 2-keto-4-methylthiobutyrate, MEP - 2-C-methyl-D-erythritol 4-phosphate, MT - monoterpenes, MVA - mevalonate, MVAPP - mevalonate-5-diphosphate, OAA - oxaloacetate, PEP - phosphoenolpyruvate, R-5-P - ribose-5-phosphate, Ru-5-P - ribulose-5-phosphate, SAH - S-adenosyl-homocysteine, SAM - S-adenosylmethionine, ST - sesquiterpenes, Tri-T - Tri-terpenes, TT - tetraterpenes.

Other abbreviations: C - cytoplasm, CP - chloroplast, CW - cell wall, M - mitochondrion, N - nucleus, PM - plasma membrane.